



RESEARCH ARTICLE

Liver Histology and Biochemistry of Exposed Newborn and Infant Rats with Experimental Aflatoxicosis

Kubilay Doğan Kılıç^{1*}, Aylin Gökhan¹, Eser Yıldırım Sözmen² and Ayşegül Uysal¹

¹Ege University Faculty of Medicine, Department of Histology and Embryology, Izmir, Turkey

²Ege University Faculty of Medicine, Department of Biochemistry, Izmir, Turkey

*Corresponding author: kubilaydk@gmail.com; kubilay.dogan.kilic@ege.edu.tr

ARTICLE HISTORY (22-203)

Received: June 17, 2022
Revised: August 10, 2022
Accepted: August 27, 2022
Published online: September 20, 2022

Key words:

Aflatoxin
Gestation
Lactation
Newborn
Infant
Rats
Liver
Food safety.

ABSTRACT

Gestational and lactational transmission of Aflatoxin B1 (AFB1) can elicit several toxic effects emphasizing the severity of aflatoxicosis. The present study aimed to investigate the genotoxic effects of prenatal and postnatal exposure to AFB1 on the livers of exposed offspring. With this aim, 50 µg/kg/body weight per day AFB1 was administered intraperitoneally (i.p.) to pregnant and lactating dam rats. Pups grouped as newborns (GD21/PND0) exposed in utero and infants exposed through breast milk (PND21) were compared with body weight measurements. Liver tissues were weighed after removal and subjected to histochemical (HC), immunohistochemical (IHC) and biochemical analyzes. The body weight and liver weight of exposed newborns were significantly lower than control ($P<0.05$). The histomorphological changes were more pronounced in exposed newborns. A decrease ($P<0.05$) in the histological score (HSCORE) of cytokeratin 19 (CK19) IHC, fetal stem/progenitor cells marker, and an increase ($P<0.05$) in the HSCORE of alpha-fetoprotein (AFP) IHC, hepatocellular carcinoma (HCC) marker, were detected in both exposed groups. Exposed newborns showed higher CK19 and AFP HSCORE than exposed infants ($P<0.05$). Both groups exhibited a low proliferation index score of proliferating cell nuclear antigen (PCNA) IHC ($P<0.05$). The high apoptotic index score of immunofluorescence (IF) staining of the terminal deoxytransferase-mediated dUTP nick-end labeling (TUNEL) method was significant in exposed newborns ($P<0.05$). Evaluation of oxidative stress and antioxidant systems revealed that tissue malondialdehyde (MDA) levels decreased in exposed newborns and increased in exposed infants ($P<0.05$), and tissue catalase (CAT) levels increased in both groups ($P<0.05$). In conclusion, the effects of AFB1 exposure during the gestational period occurred more severely, and the importance of preventing AFB1 exposure was revealed.

To Cite This Article: Kılıç KD, Gökhan A, Sözmen EY, Uysal A, 2022. Liver histology and biochemistry of exposed newborn and infant rats with experimental aflatoxicosis. *Pak Vet J*, 42(4): 453-460. <http://dx.doi.org/10.29261/pakvetj/2022.066>

INTRODUCTION

Food contamination with aflatoxin B1 (AFB1) remains one of the leading problems in the field of food safety and livestock industry, as well as in the health system and economy. Placental and breast milk transmission of AFB1 may cause mutagenic, carcinogenic, and teratogenic effects, indicating the importance of aflatoxicosis (Benkerroum, 2020; Jubeen *et al.*, 2022). The most prominent effects were associated with the high potential of AFB1 in terms of genotoxicity, both active metabolites and increased oxidative stress resulting from metabolism are accused as the main source

of mutations and DNA damage (da Silva *et al.*, 2021; Ashraf *et al.*, 2022). Since the liver is the main organ on which AFB1 acts, tissue damage is expected to occur primarily in the liver. However, the severity of acute and chronic pathologies varies according to the amount and duration of exposure and the organism exposed. Long-term studies involving newborns and infants as the most susceptible populations are needed to elucidate the effects of AFB1 exposure on baby health.

The negative effects of AFB1 on rodents have been listed in past studies as follows: liver and kidney damage, inhibition of normal growth, alterations in reproductive and developmental parameters, immunotoxicity, as well

as changes in the gut microbiota (Li *et al.*, 2022; Sobral *et al.*, 2022). For these effects, the No Observed Adverse Effect Level (NOAEL) has been reported as approximately 30 µg/kg body weight per day, and the median lethal dose (LD50) as 0.4-18 mg/kg body weight (Schrenk *et al.*, 2020). Furthermore, the consumption of staple foods containing 1 mg/kg and higher of aflatoxin or exposure to 20-120 µg/kg body weight per day for 1-3 weeks is assumed to be responsible for an acute toxic dose, thus lethality, in humans. The dam rats in the second-third trimester of pregnancy treated with AFB1 at a daily dose of 10-100 µg/kg body weight (i.m.) gave birth to newborns showing various signs of toxicities, in addition to that, the immunological parameters were significantly altered with the rats treated with 1 mg/kg body weight (i.p.) of AFB1 (World Health Organization, 2018).

Nevertheless, experimental aflatoxicosis studies examining the toxic effects of AFB1 exposure on prenatal and postnatal liver development are still needed. Based on these, we hypothesized that a daily dose of 50 µg/kg body weight (i.p. for 21 days) of AFB1 administration to pregnant and lactating dam rats would be sufficient to induce genotoxicity in exposed newborns and infants. Furthermore, we aimed to reveal this possible genotoxicity with histological and biochemical analyses. This study will shed light on experimental aflatoxicosis, involving placental and breast milk transfer of AFB1, and guide researchers. The results of this study are also expected to guide the legislators related to public health.

MATERIALS AND METHODS

Ethical approval and animals: The study was conducted by the guide of the Declaration of Helsinki of 1975 (<https://www.wma.net/what-we-do/medical-ethics/declaration-of-helsinki/>), revised in 2013, and the protocol was approved by the Ethics Committee of Ege University Local Ethics Committee of Animal Experiments (#2016- 084). All animal experiments were carried out at the Ege University Center for Research on Laboratory Animals which also provided the production and care of animals. A mixture of xylazine (Alfazyne, Ege Vet, Alfasan International BV, Netherlands) and ketamine (Alfamine, Ege Vet, Alfasan International BV, Netherlands) was administered according to body weight (bw) for the anesthesia of the animals.

Experimental design: Three adult breeder male and fifteen adult female Albino Wistar rats weighing 200-220 g were used as a parental generation. Animals were kept under a 12/12 h light/dark cycle in a controlled environment with constant room temperature (21±2°C) and humidity (50±5%) and fed ad libitum with free access to standard lab chow and tap water.

Daily vaginal smears stained with Giemsa were obtained to determine the pattern of estrus cycles of the female dams. The criteria used to distinguish the phases of the estrus cycle were as follows; Proestrus, the predominance of nucleated vaginal epithelial cells either individually or in clusters, with very few leukocytes; Estrus, the predominance of non-nucleated cornified squamous epithelial cells with large and irregular shape –

the partial presence of nucleated epithelial cells absence of leukocytes; Metestrus, a mixture of cells - clusters of non-nucleated epithelial cells and fusiform-shaped dying epithelial cells and large numbers of leukocytes, Diestrus: non-nucleated epithelial cells mostly in fusiform shape, consistent absence of cornified cells, the predominance of leukocytes (Uslu *et al.*, 2013).

Animals in the same estrus cycle were caged together. Rats were mated on the night of the Proestrus period as five females and two males per cage. On the morning of the following day, the day 0 of pregnancy that was assessed by the presence of sperm in the vaginal smear, was designated as the gestational day (GD) 0, and embryonic day (E) 0.5 indicating the morning of the day after mating was set as E0. The parturition day (GD21 or E21) was designated as postnatal day (PND) 0. For the pups of the lactation period, infants were exclusively fed with breast milk until weaning by PND21. For all groups, six newborn and infant rats from each dam were randomly assigned to the study groups indicated in the experimental design in Fig. 1.

AFB1 preparation: 1 mg of AFB1 (Biorbyt, USA) was dissolved in 1 ml of ethanol and diluted with 99 ml of distilled water (Wei and Lee, 1969). A dose of 50 µg/kg body weight per day AFB1 (i.p.) was administered to pregnant dam rats throughout the gestation period (GD0-21), and to lactating dam rats throughout the breastfeeding period (PND0-21).

Measurement of body weight and liver weight: At the end of the experiments in all groups, after the newborns and infants were weighed, the livers of the pups were removed and weighed. Then, a part of the liver tissues was kept at -20°C until they were sent to the department of medical biochemistry of our institution for biochemical investigation. The remaining liver tissues were taken into the tissue processing for microscopical investigation.

Microscopical analyses

Tissue processing: Liver tissues were fixed with 4% paraformaldehyde solution, dehydrated in ascending series of alcohol, cleared with xylene, and embedded in paraffin. Paraffin blocks were sectioned at five µm thickness for HC and IHC staining, and ten µm thickness for IF staining. The cell structure of the liver was also examined in detail with TB-stained semi-thin sections cut with an ultratome (Reichert, Austria Nr.313864) from epoxy blocks. All slides were visualized with a camera (Olympus DP72, Tokyo, Japan) attached to a light microscope (Olympus BX51, Tokyo, Japan). Digital photographs were analyzed with the Cellsens Entry program (version 1.0, Olympus Inc., Tokyo, Japan).

Histochemical staining and scoring of lesions: Paraffin sections were deparaffinized, hydrated, and stained with Haematoxylin & Eosin (H&E), Mallory Azan (MA), Periodic Acid Schiff (PAS), and Toluidine blue (TB) for histomorphological examination. All HC stainings were performed following the routine protocols of our histochemistry laboratory in accordance with the literature. A comprehensive semi-quantitative analysis was performed with the microscopical observations of HC-

stained slides, and the assessment was completed blindly by a single experienced observer. In all study groups, three slides per animal were randomly selected for each staining method and slides were examined at 100x, 200x, 400x and 1000x magnifications. The HC examination was conducted according to a grading scheme modified from past studies (Thoolen *et al.*, 2010). The grading scheme is given in Table 1. The list of microscopic observations compiled from the literature, and their scores are given in Table 2 (Thoolen *et al.*, 2010; Ali *et al.*, 2021).

Immunohistochemical staining and scoring

IHC examination: Deparaffinized sections were prepared for IHC examination in accordance with the recommendations of the manufacturers of the antibodies in the study. Sections were incubated with primary antibodies of CK19 (SantaCruz, USA sc-376176), AFP (SantaCruz, USA sc-130302), and PCNA (SantaCruz, USA sc-25280) with a dilution of 1:50. DAB was used as the chromogen and hematoxylin was used for counterstain. The presence of granular or diffuse staining of brown color was assessed as positive immunoreactivity. For all study groups, the pathological and immunohistochemical changes were evaluated by a single experienced observer in a blind fashion. All slides were randomly selected and examined under the light microscope at 400x magnification with five high-power fields per slide (hpf/s). To assess the immunoreactivity, HSCORE for CK19 and AFP, and proliferation index for PCNA were calculated as described below.

Scoring of CK19 and AFP IHC (HSCORE): Slides were evaluated semi-quantitatively to determine the intensity and the distribution of the immunoreactivity. For each slide, the intensity scale was defined as not present (0), weak but detectable (1+), distinct (2+), and intense (3+), and the HSCORE was calculated as $HSCORE = \sum Pi(i+1)$, where i is the intensity score (0-3), and Pi is the percentage of the cells showing that intensity (0-100%) (Uslu *et al.*, 2013; Kaya-Dagistanli *et al.*, 2013).

Scoring of PCNA IHC (Proliferation Index): Slides were evaluated to calculate the percentage of positive cells immunolabelled with PCNA. The proliferation index was calculated by dividing the number of labeled cells by the number of total cells and multiplying by 100 (Viswanathan *et al.*, 2015).

Immunofluorescence staining and scoring

TUNEL IF examination: Apoptotic cells were detected in the TUNEL IF method performed with the ApopTag Fluorescein In Situ Apoptosis Detection Kit (Sigma S7110 kit, CA, USA) according to the manufacturer's instructions. In the final step, the sections were incubated with DAB and counterstained with hematoxylin. For all study groups, the pathological and immunohistochemical changes were evaluated by a single experienced observer in a blind fashion. All slides were randomly selected and examined at 400x magnification on the whole section. To assess the immunoreactivity, the apoptotic index was calculated as described below.

Scoring of TUNEL IF (Apoptotic Index): Following the TUNEL IF staining, immunopositive cells were subjected

to morphometric analysis. Apoptotic cells were detected by examining the whole section on each slide, and the apoptotic index was calculated according to the following formula: $AI = (AC/AC+IC) \times 100$ (AI: Apoptotic index, AC: Apoptotic cell number, IC: Intact cell number). Results were recorded as the percentage of labeled cell numbers (Kaya-Dagistanli *et al.*, 2013).

Biochemical Analyses

Tissue homogenization: All procedures of biochemical investigations were performed in line with past literature (Sozmen *et al.*, 1994). Liver tissues were weighed and homogenized with phosphate buffer (1/10:w/v) on ice. Analyses were performed after centrifugation at 2000 G for ten minutes.

MDA measurement: The TBA-added homogenate was boiled at 100°C for 20 minutes. It was centrifuged at 2000 rpm for 10 minutes. The supernatant was measured colorimetrically at a wavelength of 532 nm. MDA was calculated as nmol/ml with the standard graph of 1,1,4,4 and the results were given as nmol/g Hb.

CAT measurement: Homogenates were diluted 1/10 with phosphate buffer. Levels were determined by the UV spectrophotometric method based on the breakdown of hydrogen peroxide by catalase. The sample was added to a freshly prepared phosphate buffer solution containing 30 mM H₂O₂. Absorbance decrease at 240 nm wavelength was read for 2 minutes at fifteen-second intervals, and the k value and enzyme amount were calculated by finding the most suitable absorbances for each analysis according to linear regressions. To standardize the results, data were given as U/g Hb enzyme activity.

Determination of protein amount: The amount of protein in the tissue was determined by the Lowry method using the bovine serum albumin standard (Lowry *et al.*, 1951).

Statistical analysis: The parameters obtained from histological and biochemical investigations were evaluated with the SPSS 23.0 package program. Following the normality analysis, a t-test was applied if the groups were independent, the Mann-Whitney U test was applied if the groups were not independent, and the significance value was accepted as $P < 0.05$.

RESULTS

Body weight and liver weight: A comparison of study groups' body weight and liver weight measurements revealed a statistically significant decrease in only exposed newborns compared to control newborns ($P < 0.05$). Statistical results are given in Fig. 2.

Histochemical examination: Control group rats showed normal histomorphological appearance according to developmental stages. The livers of AFB1 exposed rats, particularly exposed newborns, were more degenerated. The sections of exposed newborns showed partial dilatation in sinusoidal structures, loss of endothelial integrity and deterioration in hepatic cords, together with

Table 1: Grading scheme for HC examination

Grade	Severity	Proportion/Amount of affection
0	Not present or within normal levels	Null or negligible
1	Minimal remarkable, marginal	Rare, very low, very small
2	Mild, slight, weak	Few, low, small
3	Moderate, common, distinct	Several, intermediate, medium
4	Severe, intense, strong	Diffuse, high, large

Table 2: Scores for HC examination of study groups

Microscopic Observation	G1	G2	G3	G4
Alteration of hepatic architecture	0	0	4	2
Congestion	0	0	2	2
Sinusoidal dilatation	0	0	2	3
Disarray of hepatic cords	0	0	4	2
Deterioration of parenchyma	0	0	3	2
Disintegrity of vascular endothelium	0	0	3	1
Increased periportal connective tissue	0	0	2	3
Increased periportal cell assembly	0	0	2	3
Inflammatory cell infiltrate	0	0	1	2
Hematopoietic cell assembly	2	0	1	0
Hepatocyte degeneration	0	0	4	3
Cytoplasmic vacuolation	0	0	2	3
Hypereosinophilic cytoplasm	0	0	3	2
Pyknotic and fragmented nuclei	0	0	3	2
Apoptosis/single cell necrosis	0	0	3	2
Alterations in glycogen content	0	0	2	1
Megalocytosis	2	0	3	1
Binucleation	2	1	3	1

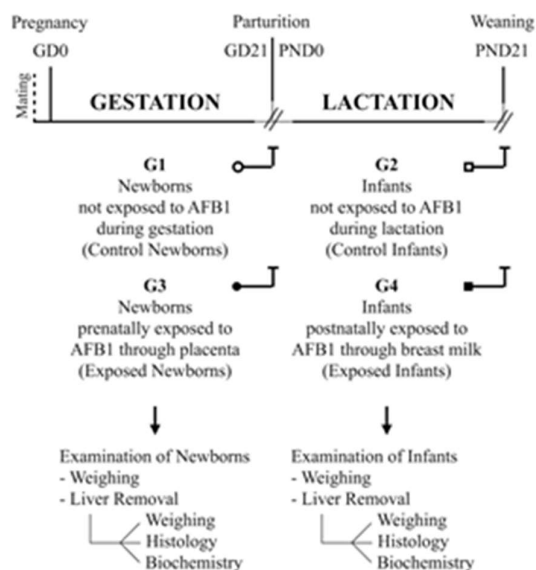
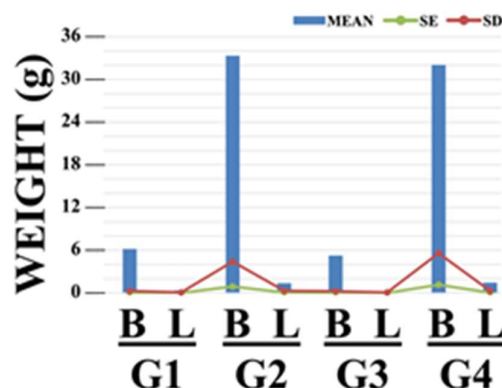
A semi-quantitative assessment from microscopic observations of H&E, MA, PAS and TB stained slides. Three slides per animal were examined for each staining. The assessment was performed over the whole slide at 100x, 200x, 400x and 1000x magnifications. H&E, Haematoxylin & Eosin; MA, Mallory Azan; PAS, Periodic Acid Schiff; TB, Toluidine blue.

the presence of hematopoietic cell populations. Moreover, in some areas of the central vein endothelium, local integrity was impaired, vacuolization and lipid-like structures increased in hepatocytes, hepatocytes with pycnotic nuclei, and multinucleated pale cell communities were detected. A slight increase in connective tissue was observed in the periphery of the central vein, with partial lymphocyte infiltration in the connective tissue in the portal areas. Similarly, in the sections of the exposed infants, enlargement in sinusoidal structures, areas with impaired integrity of the central vein, and pale hepatocytes with vacuolar structures were distinguished. In addition, collagen fibers were detected more prominently in the perivascular connective tissue areas. The representative sections are given in Fig. 3.

HSCORE: Both experimental groups, exposed newborns and exposed infants, showed a significant decrease in CK19 HSCORE and a significant increase in AFP HSCORE compared to the respective control groups ($P < 0.05$). Exposed newborns showed higher CK19 and AFP HSCORE than exposed infants ($P < 0.05$). Representative sections and statistical results are given in Fig. 4.

Proliferation index: Low scores of proliferation index were detected in both exposed newborns and exposed infants compared to the respective control groups ($P < 0.05$). Representative sections and statistical results are given in Fig. 4.

Apoptotic index: TUNEL IF immunolabelling showed positive cells around the central vein in exposed newborns, especially in areas adjacent to the endothelium.

**Fig. 1:** Timeline and design of the research with study groups (G1-4) and analyses.**Fig. 2:** Bodyweight and liver weight measurements of the study groups (G1-4). Statistical significance is mentioned in the text. B, bodyweight; L, liver weight.

Fewer TUNEL-positive cells were detected in regions other than the central zone. Although immunopositive cells were also found in exposed infants, the high apoptotic index of exposed newborns was statistically significant ($P < 0.05$). Representative sections of the TUNEL IF investigation and statistical results of apoptotic index scoring are given in Fig. 5.

MDA and CAT levels: MDA analysis results revealed a significant decrease in exposed newborns and a significant increase in exposed infants compared to the corresponding control groups ($P < 0.05$). However, CAT levels were significantly increased in both exposed newborns and exposed infants compared to the corresponding control groups ($P < 0.05$). Statistical results are given in Fig. 6.

DISCUSSION

Among the aflatoxins produced by *Aspergillus* sp., AFB1 is the most strongly associated with immunotoxicity, hepatotoxicity and teratogenicity at long-term exposure, and is attributed as the most toxic and most potent carcinogenic mycotoxin (Rushing and Selim, 2019).

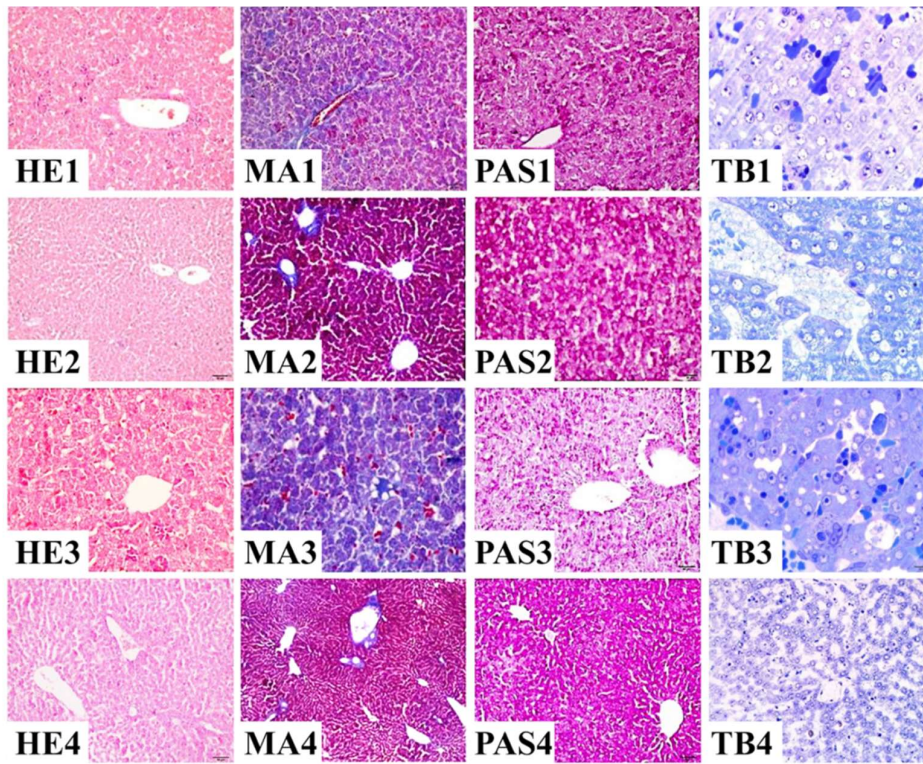


Fig. 3: Representative sections of HC investigation. Letters refer to HC stains. Numbers (1-4) refer to study groups (G1-4). Total magnification 200x for H&E, MA, and PAS, and 1000x for TB. HE, Haematoxylin & Eosin; MA, Mallory Azan; PAS, Periodic Acid Schiff; TB, Toluidine Blue.

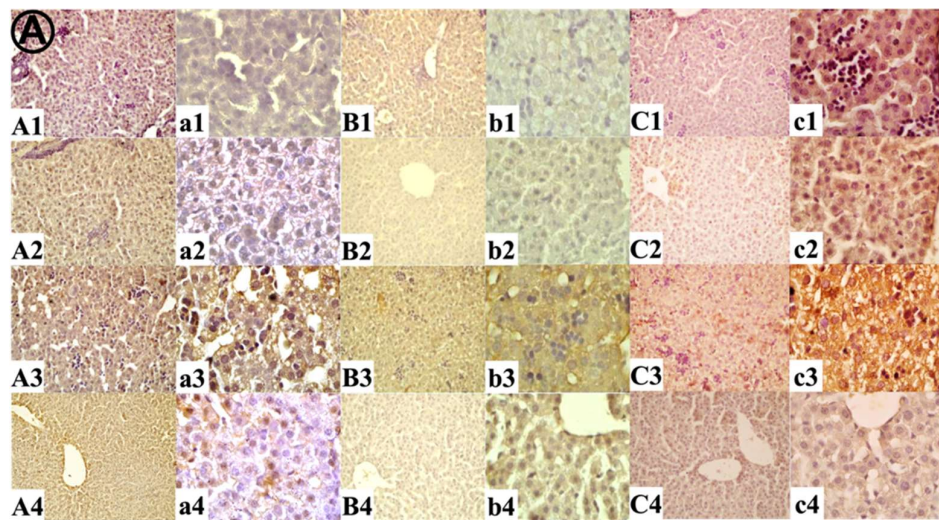
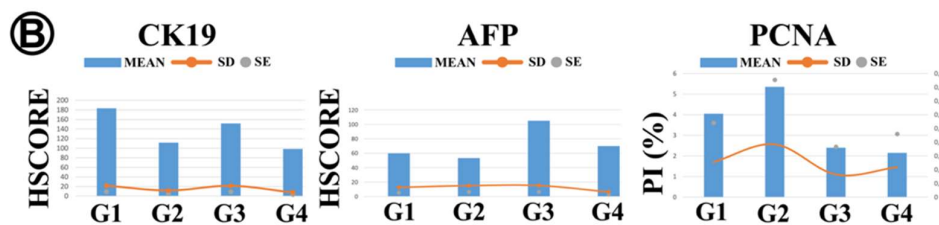


Fig. 4: Representative sections (A) and statistical results (B) of IHC investigation. A) Letters (A-C) refer to CK19, AFP, and PCNA IHC, respectively. Uppercase letters indicate 200x total magnification, lowercase letters indicate 1000x total magnification. Numbers (1-4) refer to the study groups (G1-G4). B) Statistical results of HSCORE of CK19 and AFP IHC and PI scoring of PCNA IHC. Statistical significance is mentioned in the text. CK19, cytokeratin 19; AFP, alpha-fetoprotein; PCNA, proliferating cell nuclear antigen; HSCORE, histological score; PI, proliferation index.



Aflatoxin contamination of the food may occur due to improper storage of nutrients in the pre-harvest and post-harvest periods. Considering that its toxic effect cannot be eliminated by daily cooking, it is not difficult to estimate the importance of AFB1 on the food-animal-human circle, in other words, the impacts of aflatoxicosis on the livestock and the health sector, and the economy cannot be ignored (Benkerroum, 2020; Bhatti *et al.*, 2021).

Although there is a widespread view that aflatoxins cause a slowdown in the growth rate of children, it is also stated that this result may have been overestimated due to the lack of detailed analysis (World Health Organization, 2017). Contrary to this, the statistical analysis of both body weight and liver weight from our study revealed that there was a significant decrease in both body and liver weights of AFB1 exposed newborns compared to the control

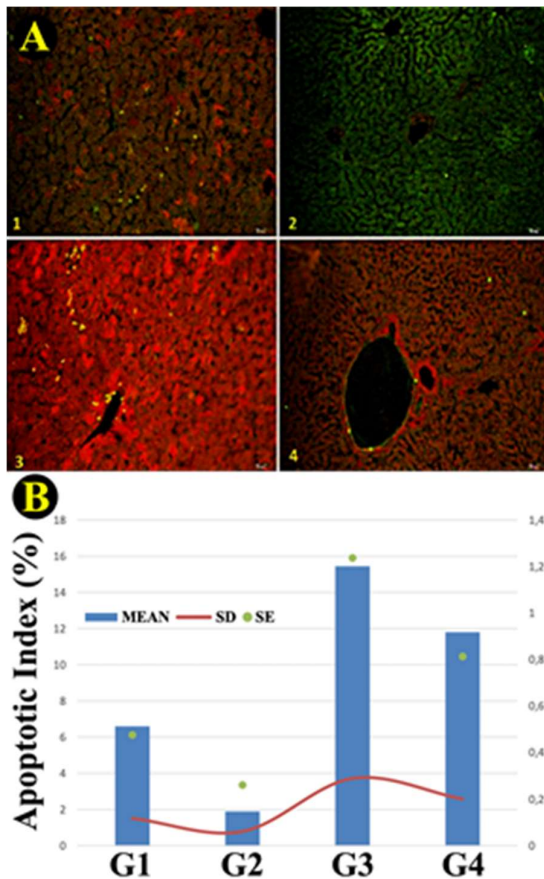


Fig. 5: Representative sections (A) and statistical results (B) of TUNEL IF investigation. A) Numbers (1-4) refer to the study groups (G1-G4). B) Statistical results of apoptotic index (%) scoring of study groups. Statistical significance is mentioned in the text.

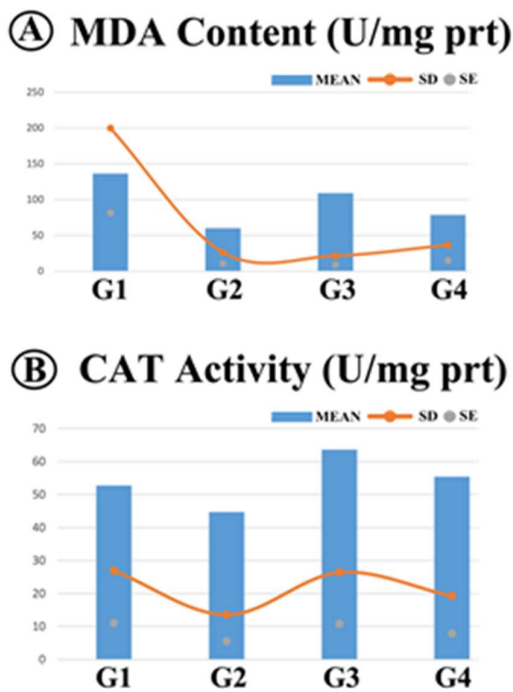


Fig. 6: Statistical results of the biochemical investigation. A) MDA analysis results. B) CAT analysis results. Numbers (1-4) refer to the study groups (G1-G4). Statistical significance is mentioned in the text. MDA, malondialdehyde; CAT, catalase.

($P < 0.05$). This finding led us to the conclusion that the dose of AFB1 in our experiment caused intrauterine growth retardation.

Listed in Group 1 by the International Agency for Research on Cancer (IARC), AFB1 is considered a human genotoxic carcinogen and is among the main causes of the development of HCC, one of the most aggressive tumors (Jubeen *et al.*, 2022). The carcinogenicity of AFB1 is mainly due to genotoxicity, the mutation-inducing effect of AFB1-DNA adducts in p53 and p21 is of particular importance (Pogribny, 2019). AFB1 at a dose of 20 $\mu\text{g}/\text{kg}$ body weight/daily (i.p. for 21 days) led to p21 overexpression in mice. As a result, the cell cycle has stopped, and apoptosis has developed. In further, animals given aflatoxin at doses of 0-100 $\mu\text{g}/\text{kg}$ body weight/daily showed impaired organ development and several defects; these results were explained by the binding of active intermediates of aflatoxins to DNA and to serum albumin, as well as inhibition of protein synthesis (Santos *et al.*, 2017; Benkerroum, 2020). The variability of enzyme levels in the liver that convert the active metabolites to inactive products has been shown to be the main reason for the difference in the development of AFB1-dependent HCC. Although the development of carcinogenesis is known to vary with species, age, exposure time, and amount, it is accepted that rats and even humans are more susceptible to AFB1-induced HCC and mice are more resistant (Santos *et al.*, 2017).

A recent study noted that data from non-oral routes of administration would not reflect the consequences of natural aflatoxin exposure due to the presence of bypassed intestinal mechanisms (da Silva *et al.*, 2021). However, we investigated this issue in our current study by administering the AFB1 intraperitoneally for every day of gestation and lactation. Indeed, our findings support past studies reporting histopathological changes including degenerative and congestive lesions of liver such as alteration of liver architecture, hepatocyte degeneration, vacuolization, necrosis, hemorrhage, fatty degeneration and centrilobular vein occlusion, as well as morphological changes such as decrease in liver weight and size (Ali *et al.*, 2021; da Silva *et al.*, 2021).

As embryonic development continues, the fetal liver bud hosts hepatoblasts. Since hepatoblasts exhibit AFP, albumin (hepatocyte marker) and CK19 (biliary marker), it was concluded that they may represent fetal liver stem cells that can repopulate both the biliary system and hepatocytes (Duncan *et al.*, 2009). It is known that the expression of AFP decreases as maturation increases, and the AFP gene is silenced after birth (Jochheim *et al.*, 2004; Tian *et al.*, 2016). AFP elevation in mature liver has been associated with malignant transformation of cells, with HCC being the most frequent type of cancer to emerge as the process progresses. In our study, we observed increased expression of AFP in both exposed newborns and exposed infants. Although we did not detect any visible cancer, we hypothesize that the elevation of AFP may be due to an increase in cells about to evolve into HCC. Suppressed proliferation as detected in our study has been observed in severe and/or chronic liver injury induced by toxicants in other studies. (Jochheim *et al.*, 2004; Duncan *et al.*, 2009; Itoh *et al.*, 2016; Tian *et al.*, 2016). In the case of impaired proliferation, both

bipotential stem/progenitor cells, which are named oval cells in rats, and biliary endothelial cells (BEC) have been reported to differentiate into hepatocytes (Duncan *et al.*, 2009). Consistent with these, we found that the proliferation index decreased, and AFP expression increased in our study. In addition to these, considering the decreased expression of CK19, we speculated that the number of stem cells expressing CK19 might have decreased, considering the decreased expression of CK19. Taken as a whole, our results seem to support other studies reporting that BEC/cholangiocytes transform into hepatocytes and contribute to repair or regeneration in liver injuries when hepatocyte proliferation is significantly inhibited (Pu and Zhou, 2022). At this point, although it is accepted that there is a difference between rats and mice, the current studies suggest that transdifferentiation of BEC to hepatocyte or stem/progenitor cell to hepatocyte might occur also in chronic liver disease in humans and that in several HCC cases the source may be related to these differentiations (Gadd *et al.*, 2020). Although it is generally accepted that a liver stem population or subpopulation exists, this area is still open to new developments. Figuring out the conditions under which liver cells will transform or what threshold of liver failure triggers the differentiation of BECs into hepatocytes will contribute to the development of appropriate biomarkers in the diagnosis and treatment of severe liver disease in the future (Russell *et al.*, 2019). In this context, the lineage tracing systems promise a very bright future.

We observed an increase in the apoptotic index calculated from the TUNEL test in both experimental groups as an expected outcome after toxic substance administration, but unexpectedly we found an increase in the antioxidant enzyme CAT in the livers of both experimental groups. More surprisingly, the lipid peroxidation end-product MDA, which we prefer to use as an oxidative marker, increased in exposed infants but not in exposed newborns. The oxidative stress markers are expected to be increased, and the antioxidant enzyme levels to be decreased after exposure to toxicants. Thus, we postulated that our inconsistent MDA and CAT analyses should have been affected by several factors.

First, regarding the duration of exposure to toxicants, while it may be considered chronic exposure when it covers the entire prenatal period, the same duration may not be considered chronic for the postnatal period. From this perspective, we hypothesized that low hepatic MDA levels in exposed newborns may result from a relatively more chronic injury to the liver than acute injury. Indeed, it has been shown that smoking could acutely increase MDA but thereafter decrease MDA even if smoking were continued, suggesting that MDA only increases in acute injury but decreases in a chronic injury (Durak *et al.*, 2020).

Second, we suspected that histological changes might not have been reflected in the biochemical test results, since our liver homogenates might have contained both damaged and healthy cells and the intensity of the damage might have varied locally. This result is consistent with the results of Sheng *et al.* (2001) who reported that prenatal and postnatal exposure to nicotine decreased hepatic MDA levels in both newborns and 10-day-old

infants, although it caused necrosis in the liver (Sheng *et al.*, 2001). In sum, we assumed that if it is planned to measure liver MDA content as a marker of oxidative stress in prenatal AFB1 exposure, attention should be paid to gestational age, still, this deduction needs to be supported by further studies.

Conclusions: In this study, the livers of newborns exposed to AFB1 during the antenatal period and of infants exposed to AFB1 through breast milk during the lactation period were compared with semi-quantitative, quantitative, and qualitative analyses. All results together made it possible to suspect a link between exposure to AFB1 and alteration in progenitor cells. The fact that the toxic effects of AFB1 exposure were more pronounced in exposed newborns in our study suggests that AFB1 may have a genotoxic potential that may affect not only living individuals but also future generations. Considering the cell density and functional diversity in the tissues, the future studies comparing different doses and exposure times with a multidisciplinary approach are still needed.

Acknowledgements: This study is a master's thesis and was supported by the Scientific and Technological Research Council of Türkiye with the TUBITAK 2211 scholarship program. We would like to express our gratitude to Ege University for its great support to the study.

REFERENCES

- Ali FAZ, Abdel-Maksoud FM, Elaziz HOA, *et al.*, 2021. Descriptive histopathological and ultrastructural study of hepatocellular alterations induced by aflatoxin B1 in rats. *Animals* 11:1-15.
- Ashraf A, Saleemi MK, Mohsin M, *et al.*, 2022. Pathological effects of graded doses of aflatoxin B1 on the development of testes in juvenile white leghorn males. *Environ Sci and Pollut Res* <https://doi.org/10.1007/s11356-022-19324-6>
- Benkerrour N, 2020. Chronic and acute toxicities of aflatoxins: Mechanisms of action. *Int J Environ Res Public Health* 17:423.
- Bhatti SA, Khan MZ, Saleemi MK *et al.*, 2021. Combating immunotoxicity of aflatoxin B1 by dietary carbon supplementation in broiler chickens. *Environ Sci Pollut Res* 35:49089-101. doi: 10.1007/s11356-021-14048-5
- da Silva JVB, de Oliveira CAF and Ramalho LNZ, 2021. Effects of Prenatal Exposure to Aflatoxin B1: A Review. *Molecules*. 26:7312.
- Duncan AW, Dorrell C and Grompe M, 2009. Stem Cells and Liver Regeneration. *Gastroenterology* 137:466-81.
- Durak I, Bingol NK, Avci A, *et al.*, 2000. Acute effects of smoking of cigarettes with different tar content on plasma oxidant/antioxidant status. *Inhal Toxicol* 12:641-7.
- Gadd VL, Aleksieva N and Forbes SJ, 2020. Epithelial Plasticity during Liver Injury and Regeneration. *Cell Stem Cell* 27:557-73.
- Jochheim A, Hillemann T, Kania G, *et al.*, 2004. Quantitative gene expression profiling reveals a fetal hepatic phenotype of murine ES-derived hepatocytes. *Int J Dev Biol* 48:23-9.
- Jubeen F, Zahra N, Nazli ZIH, *et al.*, 2022. Risk Assessment of Hepatocellular Carcinoma with Aflatoxin B1 Exposure in Edible Oils. *Toxins* 2022,14: 547. <https://doi.org/10.3390/toxins14080547>
- Itoh T, Kok CYY, Takase HM, *et al.*, 2016. Liver stem cells. In: Steinhoff G, ed. *Regenerative Medicine - from Protocol to Patient: 2. Stem Cell Science and Technology: Third Edition*. Cham, Switzerland: Springer International Publishing pp:209-40.
- Kaya-Dagistanli F, Tanriverdi G, Altınok A, *et al.*, 2013. The effects of alpha lipoic acid on liver cells damages and apoptosis induced by polyunsaturated fatty acids. *Food Chem Toxicol* 53:84-93.
- Li C, Liu X, Wu J, *et al.*, 2022. Research progress in toxicological effects and mechanism of aflatoxin B1 toxin. *PeerJ* 10:e13850.
- Lowry O, Rosebrough N, Farr AL, *et al.*, 1951. Protein Measurement with the Folin Phenol Reagent. *J Biol Chem* 193:265-75.
- Pogribny IP, 2019. Environmental Exposures and Epigenetic Perturbations. In: Boffetta P, Hainaut PBT-E of C 3rd edition. Oxford: Academic Press pp:574-84.

- Pu W and Zhou B, 2022. Hepatocyte generation in liver homeostasis, repair, and regeneration. *Cell Regen* 11:2.
- Rushing BR and Selim MI, 2019. Aflatoxin B1: A review on metabolism, toxicity, occurrence in food, occupational exposure, and detoxification methods. *Food Chem Toxicol* 124:81-100.
- Russell JO, Lu WY, Okabe H, et al., 2019. Hepatocyte-Specific β -Catenin deletion during severe liver injury provokes cholangiocytes to differentiate into hepatocytes. *Hepatology* 69:742-59.
- Santos NP, Colaço AA and Oliveira PA, 2017. Animal models as a tool in hepatocellular carcinoma research: A Review. *Tumour Biol* 39.
- Schrenk D, Bignami M, Bodin L, et al., 2020. EFSA Panel on Contaminants in the Food Chain (CONTAM), Risk assessment of aflatoxins in food. *EFSA journal Eur Food Saf Auth* 18:e06040.
- Sheng HP, Yuen ST, So HL, et al., 2001. Hepatotoxicity of prenatal and postnatal exposure to nicotine in rat pups. *Exp Biol Med* 226:934-9.
- Sobral MMC, Gonçalves T, Martins ZE, et al., 2022. Mycotoxin Interactions along the Gastrointestinal Tract: In Vitro Semi-Dynamic Digestion and Static Colonic Fermentation of a Contaminated Meal. *Toxins (Basel)* 14:1-18.
- Sozmen EY, Tanyalcin T, Onat T, et al., 1994. Ethanol Induced Oxidative Stress and Membrane Injury in Rat Erythrocytes. *Clin Chem Lab Med.* 32:741-4.
- Thoolen B, Maronpot RR, Harada T, et al., 2010. Proliferative and nonproliferative lesions of the rat and mouse hepatobiliary system. *Toxicol Pathol* 38:5-81.
- Tian L, Deshmukh A, Prasad N, et al., 2016. Alcohol increases liver progenitor populations and induces disease phenotypes in human iPSC-derived mature stage hepatic cells. *Int J Biol Sci* 12:1052-62.
- Uslu S, Uysal A, Bilir A, et al., 2013. Hepatic progenitor cell inhibition during embryonic period with high dose verapamil; liable joint to the cancer therapy. *Bratislava Med J* 114:369-75.
- Viswanathan V, Juluri R, Goel S, et al., 2015. Apoptotic index and proliferative index in premalignant and malignant squamous cell lesions of the oral cavity. *J Int oral Heal* 7:40-3.
- Wei R-D and Lee S-S, 1969. Stability of Aflatoxin B1 in Aqueous Solutions. *J Chinese Chem Soc* 16:174-82.
- World Health Organization, 2017. Evaluation of certain contaminants in food. *World Health Organ Tech Rep Ser* 1002:1-166.
- World Health Organization, 2018. Food and Agriculture Organization of the United Nations. Safety Evaluation of Certain Contaminants in Food: Prepared by the Eighty-Third Meeting of the Joint FAO/WHO Expert Committee on Food Additives (JECFA). Geneva PP - Geneva: World Health Organization.